

Transition metal substitutions, incommensurability and spin fluctuations in BaFe_2As_2 : What's different about Cu?

M. G. Kim,^{1,2} J. Lamsal,^{1,2} T. W. Heitmann,³ G. S. Tucker,^{1,2} D. K. Pratt,^{1,2} S. N. Khan,^{1,4} Y. B. Lee,^{1,2} A. Alam,¹ A. Thaler,^{1,2} N. Ni,^{1,2} S. Ran,^{1,2} S. L. Bud'ko,^{1,2} K. J. Marty,⁵ M. D. Lumsden,⁵ P. C. Canfield,^{1,2} B. N. Harmon,^{1,2} D. D. Johnson,^{1,6} A. Kreyssig,^{1,2} R. J. McQueeney,^{1,2} A. I. Goldman^{1,2}

¹Ames Laboratory, U.S. DOE, Iowa State University, Ames, IA 50011, USA

²Department of Physics and Astronomy, Iowa State University, Ames, IA 50011, USA

³The Missouri Research Reactor, University of Missouri, Columbia, MO, 65211, USA

⁴Department of Physics, University of Illinois, Urbana, IL 61801, USA

⁵Neutron Scattering Science Division, Oak Ridge National Laboratory, Oak Ridge, TN, 37831, USA and

⁶Department of Materials Science and Engineering, Iowa State University, Ames, IA 50011, USA

(Dated: December 12, 2018)

Neutron diffraction experiments show that the appearance of incommensurate spin-density wave order and the suppression of ordered magnetism in Co and Ni substituted BaFe_2As_2 appear consistent with a simple band-filling model. For Cu, however, the magnetic phase diagram does not display incommensurate order demonstrating that a rigid-band approach breaks down. Motivated by the observed differences in magnetic ordering and strong suppression of superconductivity with Cu substitution, we performed inelastic magnetic scattering measurements on $\text{Ba}(\text{Fe}_{1-x}\text{M}_x)_2\text{As}_2$ ($M = \text{Co}, \text{Cu}$) which show that the normal state spin fluctuation spectra are indistinguishable. These results suggest that impurity effects in the Fe plane play a significant role in controlling magnetism and the appearance of superconductivity.

PACS numbers: 74.70.Xa, 75.25.-j, 75.30.Fv, 75.30.Kz

The role of doping and its effects on structure, magnetism and superconductivity have become central issues in studies of the iron pnictide superconductors.[1–4] This is particularly true for transition metal (M) substitution on the Fe sites which, nominally, result in electron doping of the FeAs layers. When low concentrations of Co,[5, 6] Ni,[7, 8] Rh,[9, 10] Pt[11] and Pd[9, 10] replace Fe the structural transition temperature (T_S) and the antiferromagnetic (AFM) transition temperature (T_N) are both suppressed to lower values and split with $T_S > T_N$. [5–7, 9, 12–14] When the structural and magnetic transitions are suppressed to sufficiently low temperatures, superconductivity emerges below T_c and coexists with antiferromagnetism over some range of concentration. Moreover, for Co, Rh and Ni substitutions in BaFe_2As_2 , neutron diffraction measurements manifest a distinct suppression of the magnetic order parameter in the superconducting regime, which clearly indicates competition between AFM and superconductivity.[13–17]

Cu substituted BaFe_2As_2 , in contrast, suppresses the magnetic and structural transitions, but does not support superconductivity[2, 8] except, perhaps, below 2 K over a very narrow range in composition.[18] The dichotomy between Co and Ni substitutions on one hand, and Cu on the other, is also realized in quaternary fluoroarsenides.[19] However, for Co/Cu co-substituted samples, at a fixed non-superconducting Co concentration, the addition of Cu first *promotes* and then *suppresses* T_c . [18] It has been suggested[8, 20] that impurity effects may play an important role and, therefore, further comparative studies of Co, Ni and Cu substitutions are clearly called for and may provide important clues regarding the nature of unconventional superconductivity in the iron pnictides.

Initially, a rigid-band picture for M substitution was

widely adopted and, at least for Co substitution on the Fe site in BaFe_2As_2 , seems to adequately account for the evolution of angle-resolved photoemission spectroscopy (ARPES)[21], Hall effect, and thermoelectric power (TEP) measurements with concentration.[22] The rigid-band approach has also been used successfully to model the suppression of the AFM transition temperature and ordered moment in $\text{Ba}(\text{Fe}_{1-x}\text{Co}_x)_2\text{As}_2$ for “underdoped” samples.[17] Nevertheless, this approach neglects impurity effects and faces strong challenges from recent theoretical and experimental studies.[23–25]

Here, we report on single crystal neutron diffraction measurements of the magnetic ordering in $\text{Ba}(\text{Fe}_{1-x}\text{Ni}_x)_2\text{As}_2$ ($x \leq 0.037$) and $\text{Ba}(\text{Fe}_{1-x}\text{Cu}_x)_2\text{As}_2$ ($x \leq 0.044$). Neutron diffraction measurements, in particular the observation of incommensurate spin-density wave order, are a very sensitive probe of the nature of Fermi surface nesting in the iron pnictides and, therefore, may be used to study impurity effects as a function of the M substitution. We find that, like the Co substituted compound, Ni substitution also manifests incommensurate (IC) AFM order over a very narrow compositional range that is located at approximately half of the critical concentration for IC order in Co, as might be expected for simple band filling. However, the AFM ordering for Cu substitution remains commensurate (C) up to $x \approx 0.044$, where AFM order is absent, demonstrating that a rigid-band approach is not appropriate. The difference in magnetic ordering and the suppression of superconductivity for $\text{Ba}(\text{Fe}_{1-x}\text{Cu}_x)_2\text{As}_2$ invites a direct comparison of the inelastic magnetic scattering for Co and Cu substitutions in BaFe_2As_2 . For samples with comparable structural and magnetic transition temperatures, we show that there are no differences in the normal state spin

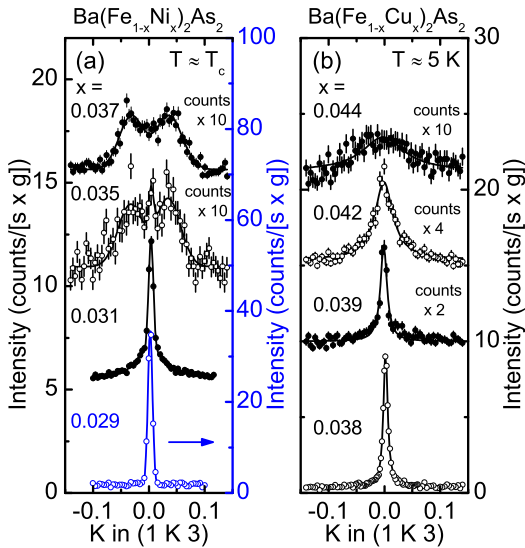


FIG. 1. (Color online) Scattering near the (1 0 3) magnetic Bragg point for (a) $\text{Ba}(\text{Fe}_{1-x}\text{Ni}_x)_2\text{As}_2$ and (b) $\text{Ba}(\text{Fe}_{1-x}\text{Cu}_x)_2\text{As}_2$. The intensities are normalized by the mass of the samples to facilitate comparisons. The lines represent fits to the data as described in the text.

fluctuation spectra. We propose that the absence of incommensurability and superconductivity for $\text{Ba}(\text{Fe}_{1-x}\text{Cu}_x)_2\text{As}_2$ arises from enhanced impurity scattering associated with Cu and note that this is also consistent with the behavior of T_c with Cu substitution in $\text{Ba}(\text{Fe}_{1-x-y}\text{Co}_x\text{Cu}_y)_2\text{As}_2$.

Single crystals of $\text{Ba}(\text{Fe}_{1-x}M_x)_2\text{As}_2$ with $M = \text{Co}, \text{Ni}$ and Cu were grown out of a FeAs self-flux using the high temperature solution growth technique described in Ref. 8 and 18. The compositions were measured at several positions on samples from each growth batch using wavelength dispersive spectroscopy. The combined statistical and systematic error on the M composition is not greater than 5%. Neutron diffraction measurements were performed on the TRIAX triple axis spectrometer at the University of Missouri Research Reactor employing horizontal collimations of $60^\circ\text{-}40^\circ\text{-}40^\circ\text{-}80^\circ$ and an incident neutron energy of 14.7 meV. The data here are described in terms of the orthorhombic indexing, $\mathbf{Q} = (\frac{2\pi H}{a}, \frac{2\pi K}{b}, \frac{2\pi L}{c})$, where $a \geq b \approx 5.6 \text{ \AA}$ and $c \approx 13 \text{ \AA}$. Samples were studied in the vicinity of $\mathbf{Q}_{\text{AFM}} = (1 \ 0 \ 3)$ in the $(\zeta \ K \ 3\zeta)$ plane, allowing the search for incommensurability along the \mathbf{b} axis ($[0 \ K \ 0]$, transverse direction) as previously found for $\text{Ba}(\text{Fe}_{1-x}\text{Co}_x)_2\text{As}_2$.^[26] Inelastic neutron scattering experiments were performed on the HB3 spectrometer at the High-Flux Isotope Reactor at Oak Ridge National Laboratory with horizontal collimation of $48^\circ\text{-}60^\circ\text{-}80^\circ\text{-}120^\circ$ and a fixed final energy, $E_f = 14.7 \text{ meV}$. Samples were aligned in the orthorhombic $(H0L)$ plane and mounted in a closed-cycle refrigerator for low temperature studies.

We have shown previously that IC AFM order is found in $\text{Ba}(\text{Fe}_{1-x}\text{Co}_x)_2\text{As}_2$ for $x \geq 0.056$, providing a measure of the effect of Co substitution on the Fermi surface.^[26] Figure 1

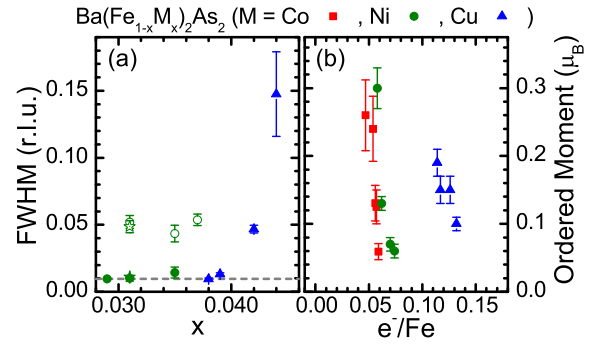


FIG. 2. (Color online) The FWHM and ordered moment for M substitutions derived from fits to the scattering data. (a) The FWHM of the magnetic peaks for Ni and Cu substitution as a function of concentration. The two symbols (open circle and star) for $\text{Ba}(\text{Fe}_{0.969}\text{Ni}_{0.031})_2\text{As}_2$ are derived from fits using a central Gaussian and either two Gaussians or a single Lorentzian, respectively, to model the tails of the scattering. The long dashed line denotes the resolution limit for our measurement. (b) The measured ordered moment calculated from the integrated intensity of the magnetic Bragg peaks as a function of the extra electron count under the assumption that Co donates 1, Ni 2, and Cu 3, extra-electrons to the d -band. The data for $\text{Ba}(\text{Fe}_{1-x}\text{Co}_x)_2\text{As}_2$ are taken from references 17 and 26.

shows the low-temperature scattering for transverse ($0 \ K \ 0$) scans through the (1 0 3) magnetic Bragg point for several Ni and Cu compositions. For $\text{Ba}(\text{Fe}_{1-x}\text{Ni}_x)_2\text{As}_2$, a transition from a C AFM structure with resolution limited magnetic Bragg peaks for $x < 0.035$, to IC AFM order for $x \geq 0.035$ is clearly demonstrated by the symmetric pair of peaks at $(1 \pm \epsilon \ 3)$ in the transverse scan. For $x > 0.037$, no long-range AFM order was observed. These data show that there is an abrupt change from C to IC AFM order in $\text{Ba}(\text{Fe}_{1-x}\text{Ni}_x)_2\text{As}_2$ at $x_c = 0.035 \pm 0.002$. The ratio (≈ 0.6) of this critical concentration to $x_c = 0.056$ for $\text{Ba}(\text{Fe}_{1-x}\text{Co}_x)_2\text{As}_2$ ^[26], seems consistent with a rigid-band picture where Ni “donates” roughly twice the number of electrons as Co.

The lines in Fig. 1(a) describe fits to the data using a single Gaussian line shape for $x = 0.029$, three Gaussians for $x = 0.035$ (to account for the presence of the dominant IC and residual C components), two Gaussians for $x = 0.037$, and a convoluted Gaussian + Lorentzian line shape for $x = 0.031$. However, we can not exclude that the tails of the scattering for $x = 0.031$ arise from a small region of IC magnetic order. The detailed description of the IC structure based on these fits is very similar for Co and Ni substitution. The incommensurability, ϵ , derived from fits to these data was 0.025 ± 0.002 reciprocal lattice units (r.l.u.), nearly identical to the value found for ϵ for Co substituted samples.^[26] Also, there is a significant broadening of the IC magnetic diffraction peaks as compared to the C magnetic peaks indicating a much reduced magnetic correlation length ($\xi \sim 60 \text{ \AA}$), again consistent with the broadening found for the Co substituted samples.^[26] The peak widths obtained from these fits are displayed in Fig. 2(a) where we see that the C component re-

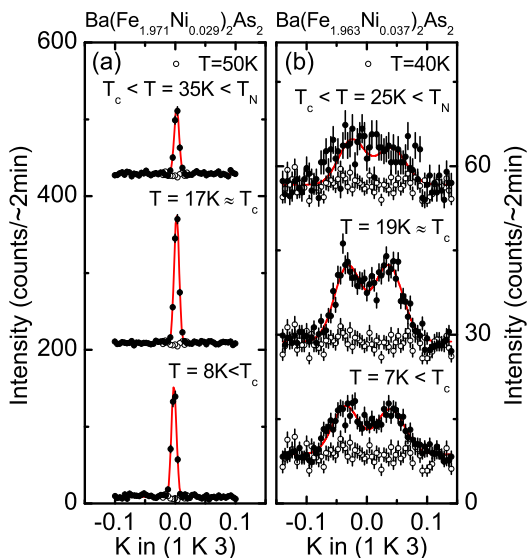


FIG. 3. (Color online) Temperature dependence of the scattering near the (1 0 3) magnetic Bragg point for $\text{Ba}(\text{Fe}_{1-x}\text{Ni}_x)_2\text{As}_2$ with (a) $x = 0.029$ and (b) $x = 0.037$. The lines represent fits to the data as described in the text.

mains resolution limited, whereas the IC peaks are approximately five times broader. Recent measurements on Ni substituted samples by Luo *et al.*[27] are consistent with these results.

The temperature dependence of the transverse (0 K 0) scans through the magnetic scattering for two superconducting samples of $\text{Ba}(\text{Fe}_{1-x}\text{Ni}_x)_2\text{As}_2$ ($x = 0.029$ and 0.037) is illustrated in Fig. 3. For both compositions, the integrated intensity of the magnetic scattering increases below T_N , reaches a maximum at the superconducting transition temperature (T_c), and decreases monotonically below T_c as observed previously for Co substituted samples,[15–17, 26] demonstrating that either C or IC magnetic order compete with superconductivity.

In striking contrast to the data presented previously for Co substitution[26] and here for Ni, Figure 1(b) shows that there is no evidence of a C-to-IC transition as a function of composition for $\text{Ba}(\text{Fe}_{1-x}\text{Cu}_x)_2\text{As}_2$. Instead, we see that the C magnetic Bragg peak is well described by a single Lorentzian line-shape that broadens strongly for $x \geq 0.039$ [see Figs. 1(b) and 2(a)], and no AFM long-range order is found for $x \geq 0.044$. To further emphasize the differences between Co, Ni and Cu substitutions, Fig. 2(b) displays the ordered magnetic moment calculated from the integrated intensity of the magnetic Bragg peaks as a function of extra electron count under the often used assumption that Co donates one, Ni donates two, and Cu donates three electrons to the d -bands. The moment has been calculated from the integrated intensity of the magnetic Bragg peaks using the C magnetic structure factor normalized by the mass of the samples as described previously.[17] Under the above stated assumption, it seems clear that Co and Ni act in a similar manner to suppress the ordered moment over a range

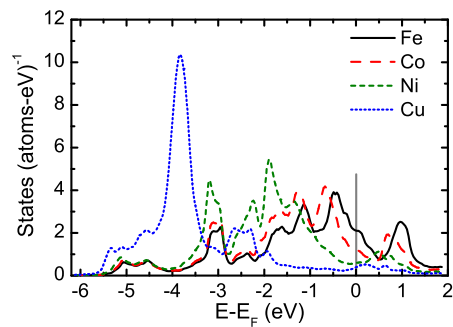


FIG. 4. (Color online) KKR-CPA calculations of the element-projected density of states for $\text{Ba}(\text{Fe}_{1-x}\text{M}_x)_2\text{As}_2$ at $e^-/\text{Fe} = 0.06$ (i.e., 6% Co, 4% Ni and 2% Cu).

of concentrations that mimics a rigid-band picture. This is clearly not the case for Cu substitution.

These differences between Co, Ni and Cu substitutions become clear when we consider how each contributes to states near the Fermi energy. To address the solute effects we employed two standard electronic structure methods, Full-potential linear augmented plane waves[28] using supercells and the Korringa-Kohn-Rostoker (Green's function) electronic-structure method with the Coherent-Potential Approximation[29] (KKR-CPA) within the parent compound unit cell. Using the KKR-CPA we calculated the electronic dispersion, density of states, total energies and substitution effects; see Refs. 29–31 for more details and examples. Our results, illustrated in Figure 4, show that the d -bands of Co and Ni show common-band, rather than rigid-band, behavior with Fe, whereas Cu exhibits split-band behavior with the d -electrons situated well below (~ 4 eV) E_F ; only s - p states participate at E_F . These results are also consistent with previous density functional theory (DFT) calculations of the partial density of states for Cu at higher concentrations.[23]

The differences found in the phase diagrams for Co and Ni substitutions on one hand, and Cu on the other are intriguing. Due to the proposed relationship between spin fluctuations and superconductivity in the iron pnictides,[1, 3, 4] we should consider whether the spin fluctuation spectrum for Cu substitution is also different from that found for Co or Ni substitution. To check this, inelastic neutron scattering measurements were performed on single-crystals of underdoped $\text{Ba}(\text{Fe}_{0.953}\text{Co}_{0.047})_2\text{As}_2$ and $\text{Ba}(\text{Fe}_{0.972}\text{Cu}_{0.028})_2\text{As}_2$. The Co sample consisted of 9 co-aligned crystals weighing a total of 1.88 grams and a total mosaic width of 1.5° full-width-at-half-maximum (FWHM), whereas the Cu sample consisted of 2 crystals with a total weight of 1.52 grams and a mosaic width of 0.6° FWHM. The two samples have similar tetragonal-orthorhombic transition temperatures [$T_S(\text{Co}) = 63$ K, $T_S(\text{Cu}) = 73$ K] and AFM transition temperatures [$T_N(\text{Co}) = 47$ K, $T_N(\text{Cu}) = 64$ K]. Bulk transport measurements show a superconducting transition for the Co substituted sample at 17 K, whereas no superconducting transition is observed in the Cu substituted sample down to 2 K.

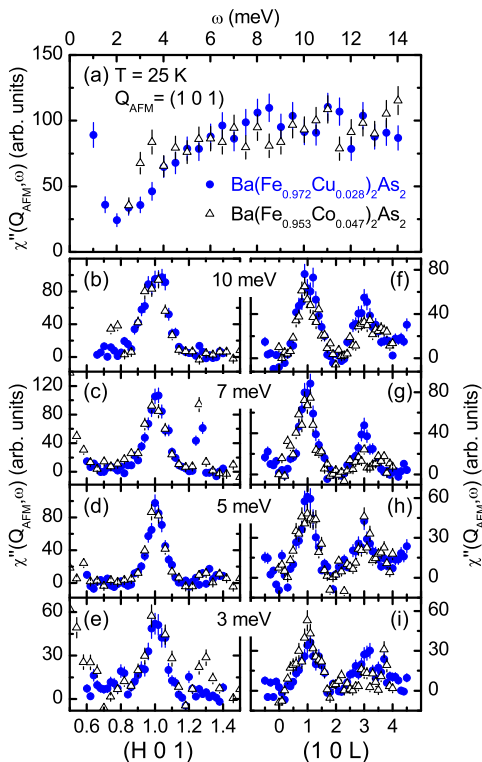


FIG. 5. (Color online) Inelastic neutron scattering from Co and Cu substituted samples. (a) Normalized dynamic magnetic susceptibility at 25 K for the both samples determined from constant- \mathbf{Q} E -scans at the (1 0 1) magnetic Bragg point as described in the text. (b)-(i) \mathbf{Q} -scans at several fixed values of the energy loss for the Co and Cu substituted samples. The feature at (1.3 0 1) results from spurious scattering not related to spin excitations.

Figure 5 summarizes our comparison of the inelastic magnetic scattering from the Co and Cu substituted samples measured at $T = 25$ K. The data are plotted in terms of the dynamic magnetic susceptibility, $\chi''(\mathbf{Q}, \omega) = [I(\mathbf{Q}, \omega) - C(\mathbf{Q}, \omega)](1 - e^{-\hbar\omega/kT})$, where $I(\mathbf{Q}, \omega)$ is the raw neutron intensity and $C(\mathbf{Q}, \omega)$ is the nonmagnetic background determined from averaged measurements of the inelastic scattering at positions well away from the magnetic signal [e.g. $\mathbf{Q} = (0.79 \ 0 \ 1.72)$ and $(0.72 \ 0 \ 1.88)$]. The data for these samples were normalized to each other using measurements of several transverse phonon peaks, and this was found to be consistent with the ratio of the masses of the two samples.

Both the constant- \mathbf{Q} energy scan measured at $\mathbf{Q}_{\text{AFM}} = (1 \ 0 \ 1)$ [Fig. 5(a)] as well as the constant- E \mathbf{Q} -scans along the [1 0 0] and [0 0 1] directions [Figs. 5(b)-(i)] show that the normal state (above T_c) dynamic susceptibility for Co and Cu substituted samples are indistinguishable. Below T_c , the spectrum of the Co substituted sample manifests a magnetic resonance feature above 4 meV (not shown here) typified by the redistribution of magnetic spectral weight from lower to higher energies in the superconducting state as observed previously by many groups.[1, 32] However, for the nonsuperconducting Cu substituted sample, the dynamic susceptibility

is temperature independent down to 5 K. The close similarity of the normal state susceptibility for single substitutions of Co and Cu show that we must look beyond the spin fluctuation spectra to understand the absence of superconductivity in $\text{Ba}(\text{Fe}_{1-x}\text{Cu}_x)_2\text{As}_2$.

We propose that the absence of incommensurability in $\text{Ba}(\text{Fe}_{1-x}\text{Cu}_x)_2\text{As}_2$ arises from enhanced scattering effects associated with the stronger impurity potential for Cu. The small incommensurability measured for Co and Ni substituted BaFe_2As_2 requires relatively well-defined features in the Fermi surface topology. Disorder due to impurity scattering can introduce spectral broadening in both energy and momentum to the extent that the magnetic structure remains C rather than IC. For example, Berlijn *et al.*, [33] point out that M substitution in the iron pnictides leads to the loss of coherence and a smearing of the Fermi surface that is relatively weak for Co substitution, but much stronger for Zn. Their DFT calculations of the configuration-averaged spectral function for disordered M substitutions did not find evidence of “localized” states but did see a significant shift in the chemical potential with Co substitution (weak impurity potential), resulting in behavior analogous to a rigid-band picture. On the other hand, Zn substitution (strong impurity potential) could no longer be viewed as a small perturbation on the system and evidences both strongly and weakly localized states. Whether or not solute effects alone are sufficient to account for the absence of an IC spin-density wave for Cu substitution deserves further study. In particular, we note that the effects of spin-disorder scattering are not accounted for in calculations done to date and likely introduce even greater smearing of the Fermi surface.

Impurity effects are expected to impact superconductivity in the iron pnictides as well. Recent theoretical work has shown that the essential elements of underdoped regions of the phase diagrams for electron-doped BaFe_2As_2 are captured by considering the effects of both inter-band and intra-band impurity scattering.[20, 34] Although impurity scattering introduced by M substitution causes pair breaking and suppresses T_c , it can be even more damaging for spin-density wave ordering so that T_N is suppressed more rapidly, allowing superconductivity to emerge at finite substitution levels. Interestingly, the phenomenological model by Fernandes *et al.*[20] indicates that the behavior of T_c for s^\pm pairing is a non-monotonic function of impurity concentration. The details of this behavior depend on the strength of the impurity potential and the ratio of the intra-band (Γ_0) to inter-band (Γ_π) impurity scattering which may vary strongly between Co and Cu substitution. Indeed, their calculations find a range in $\frac{\Gamma_0}{\Gamma_\pi}$ where T_c first increases and then decreases with impurity concentration, very similar to what has been observed for Co/Cu co-substitutions in BaFe_2As_2 .

This work was supported by the Division of Materials Sciences and Engineering, Office of Basic Energy Sciences, U.S. Department of Energy. Work at the High Flux Isotope Reactor, Oak Ridge National Laboratory, was sponsored by the Scientific User Facilities Division, Office of Basic Energy Sci-

ences, US Department of Energy.

-
- [1] D. C. Johnston, *Adv. Phys.* **59**, 645 (2010).
- [2] P. C. Canfield and S. L. Bud'ko, *Annu. Rev. Condens. Matter Phys.* **1**, 27 (2010).
- [3] J. Paglione and R. L. Greene, *Nature Phys.* **6**, 645 (2010).
- [4] G. R. Stewart, *Rev. Mod. Phys.* **83**, 1589 (2011).
- [5] A. S. Sefat, R. Jin, M. A. McGuire, B. C. Sales, D. J. Singh, and D. Mandrus, *Phys. Rev. Lett.* **101**, 117004 (2008).
- [6] N. Ni, M. E. Tillman, J.-Q. Yan, A. Kracher, S. T. Hannahs, S. L. Bud'ko, and P. C. Canfield, *Phys. Rev. B* **78**, 214515 (2008).
- [7] L. J. Li, Y. K. Luo, Q. B. Wang, H. Chen, Z. Ren, Q. Tao, Y. K. Li, X. Lin, M. He, Z. W. Zhu, et al., *New J. Phys.* **11**, 025008 (2009).
- [8] P. C. Canfield, S. L. Bud'ko, N. Ni, J. Q. Yan, and A. Kracher, *Phys. Rev. B* **80**, 060501(R) (2009).
- [9] N. Ni, A. Thaler, A. Kracher, J. Q. Yan, S. L. Bud'ko, and P. C. Canfield, *Phys. Rev. B* **80**, 024511 (2009).
- [10] F. Han, X. Zhu, P. Cheng, G. Mu, Y. Jia, L. Fang, Y. Wang, H. Luo, B. Zeng, B. Shen, et al., *Phys. Rev. B* **80**, 024506 (2009).
- [11] S. R. Saha, T. Drye, K. Kirshenbaum, N. P. Butch, P. Y. Zavalij, and J. Paglione, *J. Phys.: Condens. Matter* **22**, 072204 (2010).
- [12] C. Lester, J.-H. Chu, J. G. Analytis, S. C. Capelli, A. S. Erickson, C. L. Condon, M. F. Toney, I. R. Fisher, and S. M. Hayden, *Phys. Rev. B* **79**, 144523 (2009).
- [13] A. Kreyssig, M. G. Kim, S. Nandi, D. K. Pratt, W. Tian, J. L. Zarestky, N. Ni, A. Thaler, S. L. Bud'ko, P. C. Canfield, et al., *Phys. Rev. B* **81**, 134512 (2010).
- [14] M. Wang, H. Luo, J. Zhao, C. Zhang, M. Wang, K. Marty, S. Chi, J. W. Lynn, A. Schneidewind, S. Li, et al., *Phys. Rev. B* **81**, 174524 (2010).
- [15] D. K. Pratt, W. Tian, A. Kreyssig, J. L. Zarestky, S. Nandi, N. Ni, S. L. Bud'ko, P. C. Canfield, A. I. Goldman, and R. J. McQueeney, *Phys. Rev. Lett.* **103**, 087001 (2009).
- [16] A. D. Christianson, M. D. Lumsden, S. E. Nagler, G. J. MacDougall, M. A. McGuire, A. S. Sefat, R. Jin, B. C. Sales, and D. Mandrus, *Phys. Rev. Lett.* **103**, 087002 (2009).
- [17] R. M. Fernandes, D. K. Pratt, W. Tian, J. Zarestky, A. Kreyssig, S. Nandi, M. G. Kim, A. Thaler, N. Ni, P. C. Canfield, et al., *Phys. Rev. B* **81**, 140501(R) (2010).
- [18] N. Ni, A. Thaler, J. Q. Yan, A. Kracher, E. Colombier, S. L. Bud'ko, P. C. Canfield, and S. T. Hannahs, *Phys. Rev. B* **82**, 024519 (2010).
- [19] S. Matsuiishi, Y. Inoue, T. Nomura, Y. Kamihara, M. Hirano, and H. Hosono, *New J. Phys.* **11**, 025012 (2009).
- [20] R. M. Fernandes, M. G. Vavilov, and A. V. Chubukov, arXiv:1203.3012v1 (2012), unpublished.
- [21] C. Liu, A. D. Palczewski, R. S. Dhaka, T. Kondo, R. M. Fernandes, D. D. Mun, H. Hodovanets, A. N. Thaler, J. Schmalian, S. L. Bud'ko, et al., *Phys. Rev. B* **84**, 020509(R) (2011).
- [22] E. D. Mun, S. L. Bud'ko, N. Ni, A. N. Thaler, and P. C. Canfield, *Phys. Rev. B* **80**, 054517 (2009).
- [23] H. Wadati, I. Elfimov, and G. A. Sawatzky, *Phys. Rev. Lett.* **105**, 157004 (2010).
- [24] E. M. Bittar, C. Adriano, T. M. Garitezi, P. F. S. Rosa, L. Mendonça-Ferreira, F. Garcia, G. deM. Azevedo, P. G. Pagliuso, and E. Granado, *Phys. Rev. Lett.* **107**, 267402 (2011).
- [25] G. Levy, R. Sutarto, D. Chevrier, T. Regier, R. Blyth, J. Geck, S. Wurmehl, L. Harnagea, H. Wadati, T. Mizokawa, et al., arXiv:1203.5814v1 (2012), unpublished.
- [26] D. K. Pratt, M. G. Kim, A. Kreyssig, Y. B. Lee, G. S. Tucker, A. Thaler, W. Tian, J. Zarestky, S. L. Bud'ko, P. C. Canfield, et al., *Phys. Rev. Lett.* **106**, 257001 (2011).
- [27] H. Luo, R. Zhang, M. Laver, Z. Yamani, M. Wang, X. Lu, M. Wang, Y. Chen, S. Li, S. Chang, et al., arXiv:1203.2759v1 (2012), unpublished.
- [28] P. Blaha, K. Schwarz, G. K. H. Madsen, D. Kvasnick, and J. Luitz, *Wien2K: An Augmented Plane Wave + Local Orbitals Program for Calculating Crystal Properties* (TU Wien, Austria, 2001).
- [29] D. D. Johnson, D. M. Nicholson, F. J. Pinski, B. L. Gyorffy, and G. M. Stocks, *Phys. Rev. Lett.* **56**, 2088 (1986).
- [30] A. Alam and D. D. Johnson, *Phys. Rev. B* **80**, 125123 (2009).
- [31] A. Alam, B. Kraczek, and D. D. Johnson, *Phys. Rev. B* **82**, 024435 (2010).
- [32] M. D. Lumsden and A. D. Christianson, *J. Phys. Condens. Matter* **22**, 203203 (2010).
- [33] T. Berlijn, C. H. Lin, W. Garber, and W. Ku, arXiv:1112.4858v2 (2011), unpublished.
- [34] M. G. Vavilov and A. V. Chubukov, *Phys. Rev. B* **84**, 214521 (2011).